On accurate capacitance characterization of organic photovoltaic cells

J. A. Carr[1] and S. Chaudhary[1,2,a)]
[1]*Department of Electrical and Computer Engineering, Iowa State University, Ames, Iowa 50011, USA*
[2]*Department of Materials Science Engineering, Iowa State University, Ames, Iowa 50011, USA*

(Received 26 March 2012; accepted 2 May 2012; published online 21 May 2012)

Capacitance measurements, widely used to characterize numerous semiconductor properties, have been recently adopted to characterize organic photovoltaic (OPV) devices. It is known that certain challenges are associated with capacitance measurements. Of upmost importance is the employment of a proper measurement model (series or parallel). Owing to larger capacitive impedances and low series resistances, the parallel model is typically employed in inorganics. However, we find that for characteristically thinner organic films, a hybrid model should be used. We highlight the inconsistencies in OPV literature due to indiscriminate usage of parallel model and show how proper model selection can rectify any artifacts. © *2012 American Institute of Physics*. [http://dx.doi.org/10.1063/1.4720403]

Capacitance spectroscopy has been employed to study semiconductor properties for many years. Recently, these techniques have been adopted by the organic photovoltaic (PV) community to probe device aspects such as doping density,[1–3] deep trap states,[4–6] carrier mobility,[3] and active layer thickness.[7] It is well understood that these measurements can be very sensitive and are plagued by issues such as high impedances, leaky capacitances, and noisy cabling. Of upmost importance in maintaining reliable measurements is the selection of the proper model (e.g., parallel, series, or multiple parameters) during the measurement process. A conventional measurement employs the equivalent circuit shown in Fig. 1(a), where R_s represents the series resistance, R_p the parallel resistance, and C the capacitance. With three unknowns, measurements must be taken at two frequencies, and complex equations must be solved to find the capacitance and its associated resistances; see Ref. 8 for example. For simplicity, this equivalent circuit can be accurately modeled by either the series (highlighted by blue, solid box) or parallel (highlighted by red, dashed box) segment, depending on which portion dominates as per the capacitance, resistances, frequency, etc. In a typical solar cell, the series resistance is expected to be quite small and the parallel resistance quite large. Therefore, for large capacitive impedances, the parallel portion overshadows that of the series and dominates the measurements. In this case, the parallel model gives an accurate approximation of the equivalent circuit. In contrast, as the magnitude of capacitive impedance approaches that of the series resistance, the series model gives the most accurate approximation. Within the inorganic community, parallel parameters are typically employed. Owing to smaller series resistances and larger capacitive impedances, this parallel model remains accurate over the usual frequencies employed (e.g., 10 Hz–2 MHz). In this report, we show this detail is not directly transferrable to organic PV cells—the parallel parameters cannot be indiscriminately used. When comparing organic and inorganic cells with similar contact area, our data shows series resistances are typically two or more times higher and capacitive impedances three or more times lower in the organic devices. This moves the transition from the parallel model to the series model to lower frequencies—which can be within the range of interest. Thus, a hybrid of the two models must be employed to accurately measure the capacitance over the frequency range of interest. We show, if the improper parameters are used, geometric capacitances are underestimated, deep trap states are overestimated, and general conclusions are greatly misinterpreted. Although model choice may be a known concept, we find several evidences of improper model usage within the organic PV literature and highlight the inaccuracies they create.

As an initial example, we first turn to the capacitance versus frequency (CF) measurement of a Phenyl-C_{61}-butyric acid methyl ester (PCBM) only device (characterization details can be found in the supplementary material[15]). PCBM is a fullerene derivative of the C_{60} (or C_{70}) buckyball that shows no Mott-Schottky (MS) or deep-trap capacitive behavior with indium tin oxide (ITO) and aluminum contacts.[4] Thus, a flat capacitive response with respect to frequency and voltage is expected. This response represents a geometric capacitance, $C_g = \epsilon A/t$ ($\epsilon \equiv$ the permittivity, $A \equiv$ contact area, and $t \equiv$ thickness), in which only the dielectric is contributing. Fig. 1(b) displays the CF spectra of one such device. One immediately notes the geometric capacitance (horizontal gray at ca. 6.5×10^{15} $1/F^2$ according measured thickness of ca. 35 nm, $A = 0.1256\,cm^2$ and $\epsilon = 3.9$) requires both models to be accurately represented between 100 Hz and 1 MHz—a typical frequency range of interest as it reaches from near the Fermi level[9] to above the deep trap profile.[4,5] For those frequencies below 7.5 kHz, the parallel parameters gave the best measurement as high impedances of the parallel portion of the circuit overshadow that of the series component and dominate the voltage divider. Between 7.5 kHz and 100 kHz both models gave a good approximation, differing by less than 1%. At frequencies above 100 kHz the series model gave the best approximation. At these frequencies, the parallel impedance-combination of R_p and C falls rapidly owing to the lowering of the capacitive impedance. As this impedance becomes comparable with R_s, the series resistance becomes significant and can no longer

a)Author to whom correspondence should be addressed. Electronic mail: sumitc@iastate.edu. Tel.: 515 294 0606.

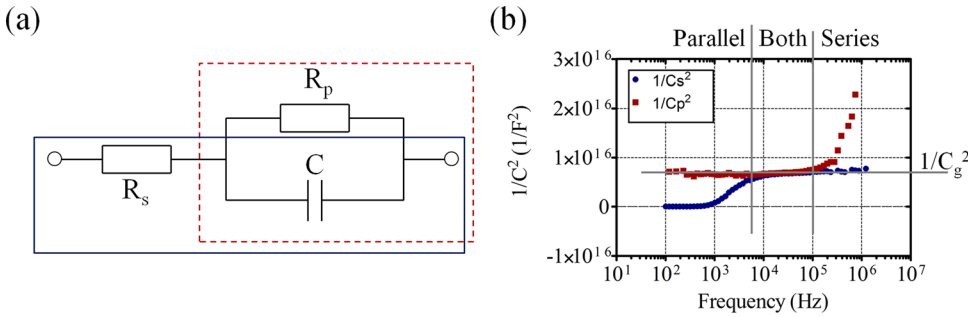

FIG. 1. (a) Simple equivalent circuit for small signal measurements. Any lead inductance is neglected here. The series approximation is highlighted by a solid blue box and the parallel by a dashed red box. (b) Capacitance ($1/C^2$) versus frequency characteristics of a PCBM only device. Both C_s and C_p parameters are shown. The calculated geometric capacitance ($1/C_g^2$) is highlighted by a gray line.

be ignored. The large parallel resistance, however, acts as a current divider and, with sufficiently small capacitive impedances, can be neglected. We note the typically thin active layer of organic films (ca. 100–200 nm) gives a larger capacitance, which causes this transition from the parallel to series to emerge at much lower frequencies than their inorganic counterparts. Frequencies below 100 Hz gave dissipation factors as high as ca. 50, indicating a very leaky capacitor whose measurement is most likely overwhelmed by noise. Above 2 MHz it is expected that the series model will continue to dominate. The PCBM device data illustrates the notion that indiscriminately using a parallel approximation across the spectrum does not transfer to organics.

The above directly translates to bulk heterojunction (BHJ) devices comprising a 1:1 weight ratio of poly(3-hexylthiophene) (P3HT):PCBM. Device fabrication details can be found in the supplementary material.[15] Fig. 2(a) plots C versus F for one such device. A pattern similar to the PCBM only device emerges, where lower frequencies favor the parallel approximation, higher frequencies favor the series, and those in-between can be estimated by either. One notes the parallel model still gives relatively reasonable values at higher frequencies. However, these values differ from the series model by anywhere between 1 and nearly 200% for this device. The choice of which of these models is most accurate is convoluted by the fact that, unlike PCBM only devices, the polymer adds a doping and deep-trap profile.[2,4,5,10] Thus, the expected capacitance may be unknown. However, at sufficiently high frequencies, the demarcation energy at which neither mobile charges nor trap states respond can be surpassed, and only the dielectric contributes to the capacitance. Thus, the geometric capacitance should be expected. We found this frequency experimentally to be ca. 1.5 to 2 MHz depending on the particular device. Qualitatively, the energy corresponding to this frequency range makes sense as it is nearing or slightly less than the equilibrium Fermi-level of P3HT (ca. 0.33 eV with doping ca. 1×10^{16}–1×10^{17} cm^{-3} as determined by 1 MHz capacitance versus voltage (CV) analysis[11]). We further confirm this geometric capacitance by applying a large (−2 VDC) reverse bias along with the entire small-signal frequency spectra in order to fully deplete the active layer—the same C_g was obtained for all frequencies at −2 VDC. Keeping this geometric capacitance in mind, the series model gave the most accurate approximation above 1.5 MHz. Further, we note that only the series capacitance reaches a plateau at these frequencies, while the parallel capacitance continues to drop. Extrapolating back, this indicates that the series model should be used for all frequencies greater than 11 kHz in these particular devices. This has two main implications for common applications of capacitance measurements: (i) C_g and thickness measurements, and (ii) determination of deep trap profiles. Both will be discussed in detail later in this report.

Of course, the boundaries at which the model must change are highly dependent on the device. Smaller capacitances, as well as series resistances, can push the parallel to series transition into higher frequencies. With a sufficiently low capacitance and R_s combination, the change may not even be noticed within the define frequency range, as is typically the case with silicon cells. A well known technique for monitoring model choice is to track the magnitude of the impedance.[12] Fig. 2(b) shows the magnitude of impedance versus frequency for the 1:1 BHJ device studied in Fig. 2(a). The general guidelines which are typically used are (i) the parallel approximation for $|Z| > 10\,k\Omega$, the series approximation for $|Z| < 1\,k\Omega$, and either for $1\,k\Omega < |Z| < 10\,k\Omega$. Fig. 2(b) shows good agreement with these guidelines.

We next turn to the literature and some of our own data to highlight inconsistencies generated by improper model usage. These inconsistencies seem to have led and, in the future, may lead to incorrect data, misinterpreted conclusions, or both. In a recent report by Li *et al.*, capacitance

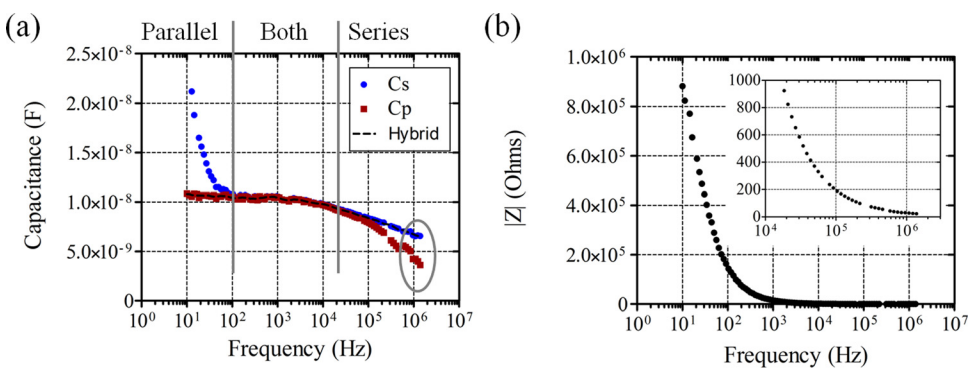

FIG. 2. (a) Capacitance versus frequency characteristics of a typical P3HT:PCBM (1:1) BHJ PV device. The ellipse highlights the differences in the geometric capacitance obtained by each model. (b) Impedance versus frequency plots showing an exponential decrease in the impedance magnitude. The inset magnifies the 10 kHz–1.5 MHz regime where |Z| drops below 1 kΩ.

techniques were used to simultaneously measure carrier density and mobility in organic semiconductors.[3] Although we generally agree with their method, we find inconsistencies in the measured geometric capacitance and the conclusions directly drawn from it. In the report, P3HT only films were characterized by CV method (−3.0 V to +0.5 V) at different frequencies (100 Hz–1 MHz). The authors found that at frequencies of 10 kHz and above, the film did not exhibit a MS response. This indicates that 10 kHz is the boundary above which mobile charges as well as trap states cannot respond, and only the geometric capacitance is measured. From this, one is left to draw the conclusion that CV and other capacitance measurements (CF, deep-level transient spectroscopy, etc.) should be conducted at frequencies lower than 10 kHz. Qualitatively, this conclusion seems implausible as the demarcation energy of 10 kHz is ca. 0.477 eV ($E_\omega = E–E_{HOMO} = kTln(\omega_0/\omega)$[13] with ω_0 estimated at $1 \times 10^{12}\ s^{-1}$), which is nearly 0.1 eV above the Gaussian center of the deep trap profile in P3HT films.[4,5] Thus, at 10 kHz, one would expect these lower lying trap states and mobile charges to respond.[11] Further, our data does not support this 10 kHz conclusion as we see MS behavior for frequencies as high as 1 MHz on P3HT only devices. As a possible explanation for this discrepancy, we explored the differences between the series and parallel approximations for CV data between 100 Hz and 1 MHz. As shown in Fig. 3(a), the models give an indication of much different device behavior at 1 MHz on our cells, with the series approximation showing MS behavior and parallel showing only a dielectric response. Here, the impedance magnitude indicates that the series model is more accurate. We note this particular P3HT device did not show low impedances (i.e., <1 kΩ) until ca. 300 kHz owing to a slightly smaller capacitance than that of the referenced work. As further evidence that the parallel parameters give an incorrect depiction of device behavior, we turn to the reverse bias region (−2 VDC). Here, the layer is fully depleted, and we clearly see the parallel model underestimates the geometric capacitance by ca. 250%. Thus, Fig. 2 shows that, for a typical P3HT device, frequencies as high as 1 MHz may still be valid for capacitance spectroscopy, and the currently published 10 kHz data is most likely the result of model misinterpretation. The exact uppermost usable frequency will be dependent on the material's Fermi level and thus can change from device to device. P3HT doping has been reported in the range of 10^{15}–$10^{17}\ cm^{-3}$, from which the Fermi level can be estimated to sit at 0.36 eV above the valence band or lower. This corresponds to freeze out frequencies of ca. 900 kHz or higher. Even doping profiles as low as $10^{14}\ cm^{-3}$ still give a Fermi level of ca. 0.42 eV or a ca. 100 kHz upper frequency. The above finding has further implications for the method of measuring capacitance to find active layer thickness. We have seen the improper model can underestimate C_g by as much as 300%. As a result, thickness can be significantly overestimated if the model is not properly adjusted.

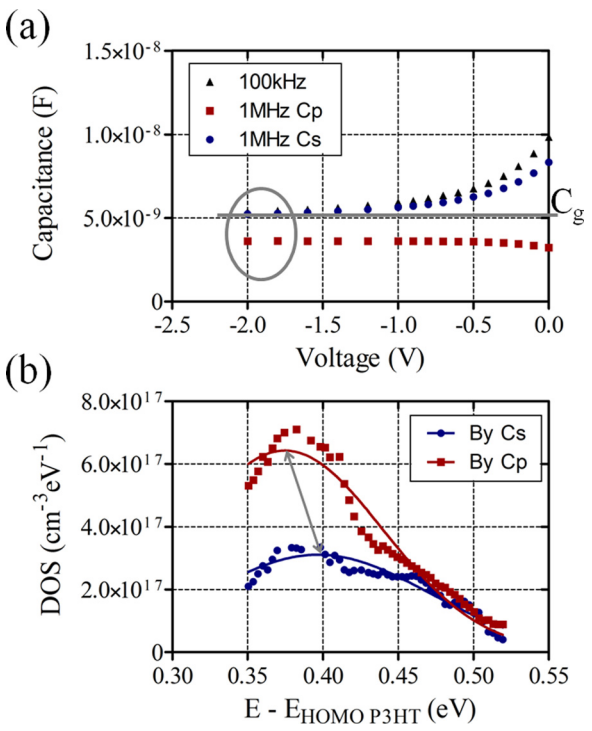

FIG. 3. (a) Capacitance versus voltage characteristics for P3HT only device at 100 kHz and 1 MHz. The calculated geometric capacitance (C_g) is highlighted by the horizontal line. The differences in the geometric capacitance obtained by the models are shown within the circle. (b) Density of trap states versus demarcation energy for P3HT:PCBM (1:1) device. The arrow shows the shift in the Gaussian amplitude and central energy between the two models.

Next, we look at the determination of deep-trap density of states (dTDOS) in organic cells. This method, which is detailed elsewhere,[4] combines CV with CF characterization to sweep through the bandgap and map defects states. As previously highlighted, the series model gives the best approximation for 1:1 BHJ based devices at higher frequencies (10 kHz to 2 MHz). The demarcation energies of these higher frequencies range from 0.477 eV to 0.339 eV. One immediately notes that this is over the range of the reported Gaussian deep-defect profile.[4,5] By comparing these models in Fig. 2(a), a large difference in slope is readily apparent. Thus, as highlighted in Fig. 3(b), if the improper model is employed, the dTDOS magnitude and distribution center can be over- and under-estimated, respectively. Using the parallel approximation, we find N_t to be overestimated by ca. 110% and the central energy to be underestimated by about 20 meV.

Lastly, we investigate a 2008 report by Jarosz.[14] In this report, the author casts doubts on MS analysis of organic planar heterojunction cells. Although we do not question the report in its entirety, we review a single plot displaying C versus F as a function of reverse bias. Here, the author correctly expects the measured frequency-dependent capacitance to decrease with an applied reverse bias. More generally stated, as the reverse bias is increased, the active-layer begins to deplete, and the capacitance at all frequencies decreases to approach the geometric capacitance. The report, however, finds an increase in capacitance with reverse bias for frequencies less than ca. 400 Hz and draws doubts on MS analysis in their cells. Although we cannot state whether MS analysis is valid or not on Jarosz's planar cells, we can highlight how improper model employment could cause one to incorrectly reach the same conclusion—even on P3HT:PCBM BHJ cells. Fig. 4 shows 1:1 BHJ CF analysis as a function of applied DC reverse bias for both the series (Fig. 4(a)) and parallel (Fig. 4(b)) models. The series model

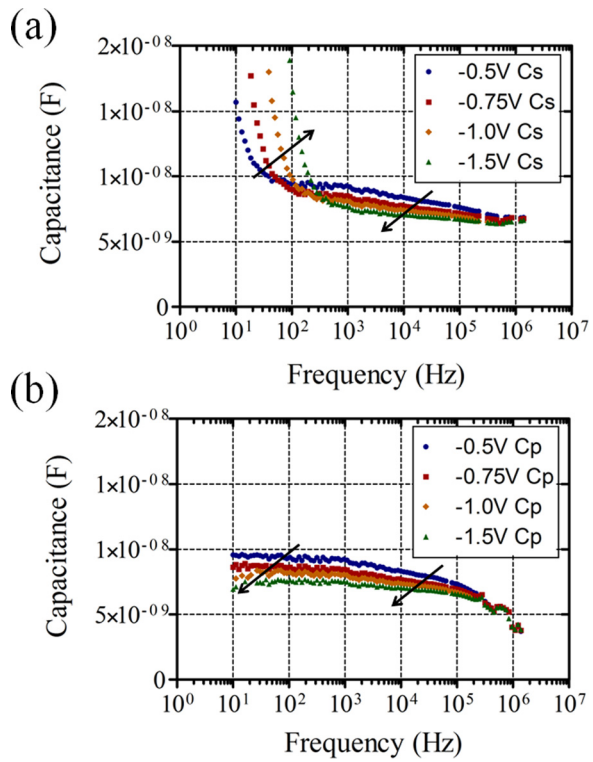

FIG. 4. Capacitance versus frequency as a function of reverse bias for (a) the series model and (b) the parallel model. The arrows indicate the direction of increasing reverse bias.

closely represents the data of the aforementioned report. This artifact arises as a direct result of the series approximation. As frequency decreases, the capacitance impedance increases and the parallel portion of circuit Fig. 1(b) dominates. By continuing to monitor the series portion, the true capacitance measurement is lost. The parallel model removes this artifact and gives the expected response. Hence, by monitoring only the series model, one might reach improper conclusions owing to inaccurate data.

Herein, the capacitance model choice was reviewed in an effort to improve capacitance measurements on organic PV cells. Although series versus parallel model selection may be a known issue, we find evidences in the literature that it is being overlooked within the organic PV community. Owing to higher series resistances and lower capacitance impedances, we find the parallel approximation cannot be indiscriminately used over the frequency range of interest. Most importantly, we find improper model employment can cause discrepancies in the geometric capacitance by as much as 300%, discrepancies in the TDOS by as much as 110%, and, more in general, misinterpreted conclusions. Our work shows that while performing capacitance characterization, it is critical to monitor the impedance magnitude and correspondingly employ the appropriate capacitive circuit model.

We thank Iowa Power Fund from the State of Iowa's Office of Energy Independence, and National Science Foundation (Award No. ECCS–1055930) for financial support. We thank Mehran Samiee Esfahani for providing us with sample silicon PV capacitance data and for helpful conversations.

[1]A. B. Guvenc, E. Yengel, G. Wang, C. S. Ozkan, and M. Ozkan, Appl. Phys. Lett. **96**, 143301 (2010).
[2]G. Dennler, C. Lungenschmied, N. S. Sariciftci, R. Schwödiauer, S. Bauer, and H. Reiss, Appl. Phys. Lett. **87**, 163501 (2005).
[3]J. V. Li, A. M. Nardes, Z. Liang, S. E. Shaheen, B. A. Gregg, and D. H. Levi, Org. Electron. **12**, 1879–1885 (2011).
[4]P. P. Boix, G. Garcia-Belmonte, U. Munecas, M. Neophytou, C. Waldauf, and R. Pacios, Appl. Phys. Lett. **95**, 233302 (2009).
[5]K. S. Nalwa, R. C. Mahadevapuram, and S. Chaudhary, Appl. Phys. Lett. **98**, 093306 (2011).
[6]A. Sharma, P. Kumar, B. Singh, S. R. Chaudhuri, and S. Ghosh, Appl. Phys. Lett. **99**, 023301 (2011).
[7]C. Lungenschmied, S. Bauer, R. Schwodiauer, S. Rodman, D. Fournier, G. Dennler, and C. J. Brabec, J. Appl. Phys. **109**, 044503 (2011).
[8]K. J. Yang and C. Hu, IEEE Trans. Electron Devices **46**, 1500 (1999).
[9]M. J. Deen, M. H. Kazemeini, Y. M. Haddara, J. Yu, G. Vamvounis, S. Holdcroft, and W. Woods, IEEE Trans. Electron Devices **51**, 1892 (2004).
[10]M. S. A. Abdou, F. P. Orfino, Y. Son, and S. Holdcroft, J. Am. Chem. Soc. **119**, 4518 (1997).
[11]L. Kimerling, J. Appl. Phys. **45**, 1839 (1974).
[12]*Agilent Impedance Measurement Handbook, 4th edition* (Agilent Technologies, 2009).
[13]S. S. Hegedus and W. N. Shafarman, Prog. Photovoltaics **12**, 155 (2004).
[14]G. Jarosz, J. Non-Cryst. Solids **354**, 4338 (2008).
[15]See supplementary material at http://dx.doi.org/10.1063/1.4720403 for characterization details and for device fabrication details.